MHD Modeling of CHI

Xianzhu Tang
Plasma Theory Group, Theoretical Division
Los Alamos National Laboratory
Email: xtang@lanl.gov

September 9, 2002

Overview

- Grad-Shafranov equilibrium modeling.
  - Helicity and energy balance.
- Resistive steady state.
  - Unlike high-S Ohmic discharges, resistive steady state gives significantly different answer from Grad-Shafranov equilibrium modeling.
  - Reason: plasma flow scales with externally imposed voltage, not parallel resistivity.
  - Consequence: plasma inertia and viscous forces induce $\mathbf{j}_\perp$. Small $\mathbf{j}_\perp$ brings strong poloidal localization of large parallel current on a flux surface.
- 3D kink instability and nonlinear saturation.
- Transient CHI for secondary current drive.

Open field line Grad-Shafranov Equi.

- Magnetic coordinates for open field lines,

  $$\mathbf{B} = \nabla\psi\times\nabla\theta+\nabla\varphi\times\nabla\chi(\psi,t) = G(\chi)\nabla\varphi+\nabla\varphi\times\nabla\chi.$$

  At electrode surfaces, $\mathbf{B}\cdot\mathbf{n} > 0, \theta = 0; \mathbf{B}\cdot\mathbf{n} < 0, \theta = 2\pi$.

- Grad-Shafranov equation is closed by specifying the parallel current from resistive Ohm's law,

  $$\frac{dG}{d\psi} = \frac{\mathcal{V}(\psi)}{q(\psi)\mathcal{R}(\psi)};\ \ \mathcal{R}(\psi) \equiv \int_0^{2\pi} \frac{\eta B^2}{\mathbf{B}\cdot\nabla\varphi} d\theta$$

- Helicity and energy balance ($\nabla p = 0$)

  $$\begin{aligned} \mathcal{V}(\psi) &= -4\pi^2 q(\psi)\eta_{\|}(G+\iota I)k_n; \\ \mathcal{V}(\psi)\frac{dG}{d\psi} &= 4\pi^2\eta_{\|}(G+\iota I)k_n^2. \end{aligned}$$

  Net parallel current $k_n = -dG/d\chi$.
  G and I are poloidal and toroidal plasma current.

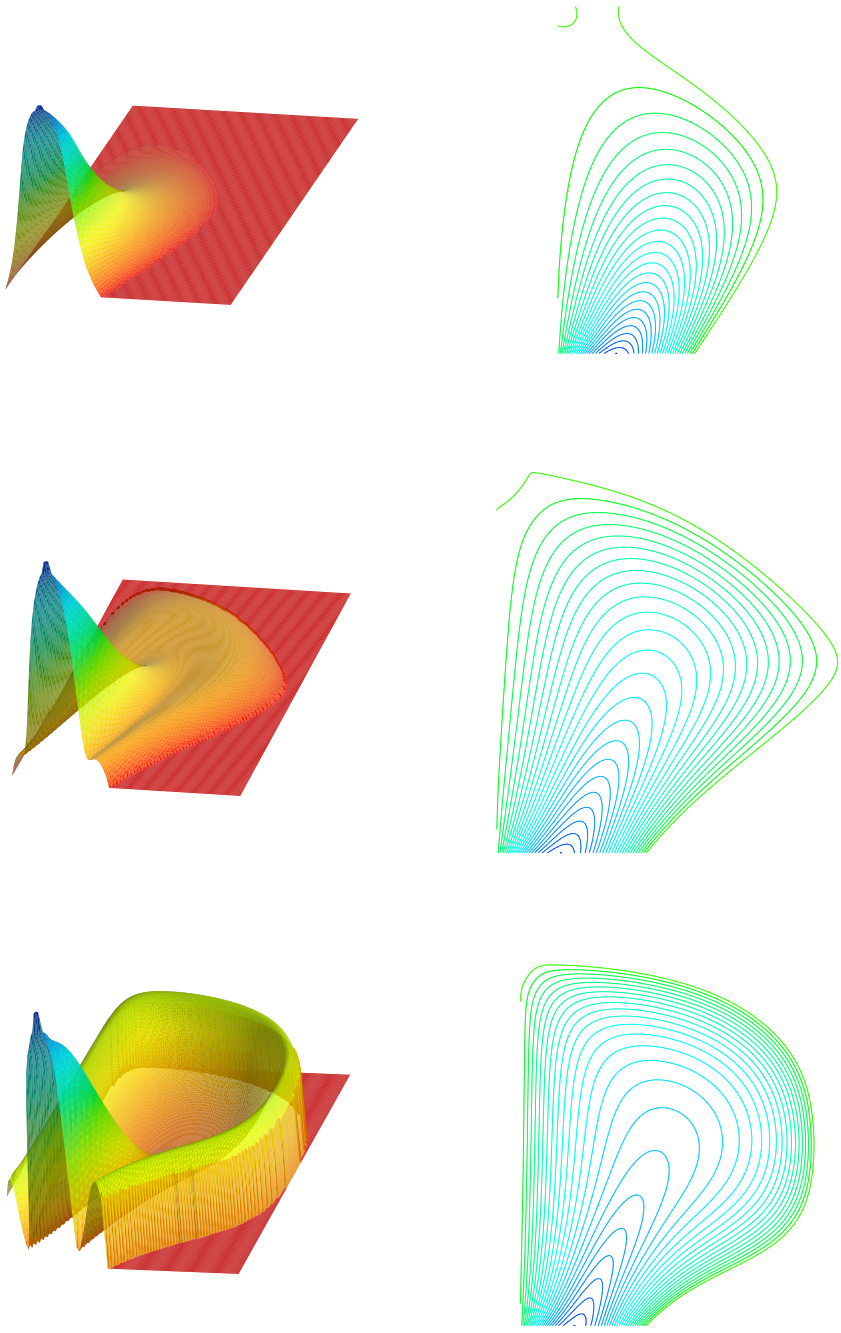

Figure 1: Surface plot of RJ_φ and contour plot of ψ (top $\mathcal{V} = -1$; middle $\mathcal{V} = -2$; bottom $\mathcal{V} = -4$.)

Resistive Steady State: Flow

- In a resistive steady state, CHI plasma has a purely electrostatic E field $\mathbf{E} = -\nabla\Phi(\psi,\theta)$, that is significantly modified by quasi-neutrality potential.

- Without plasma flow, CHI won't even work
  ($\mathbf{E} = -\nabla\Phi(\psi,\theta)$ can not drive toroidal current)

$$(\mathbf{v}\times\mathbf{B})\cdot R\nabla\varphi = \eta j_\varphi.$$

- CHI plasma flow is $\mathbf{E}\times\mathbf{B}$ and scales with $\mathcal{V}$,

$$\mathbf{v}_{\mathbf{E}\times\mathbf{B}} = \nabla\Phi(\psi,\theta)\times\mathbf{B}/B^2,$$

  Dissipative (η and ν) corrections are negligible,

$$v'_\perp \sim \max(S^{-1}\frac{v_{\mathbf{E}\times\mathbf{B}}}{v_A}v_{\mathbf{E}\times\mathbf{B}}, H^{-2}v_{\mathbf{E}\times\mathbf{B}}).$$

  Hartmann number H : $H^2 \equiv SRe\frac{v_{\mathbf{E}\times\mathbf{B}}}{v_A}$.

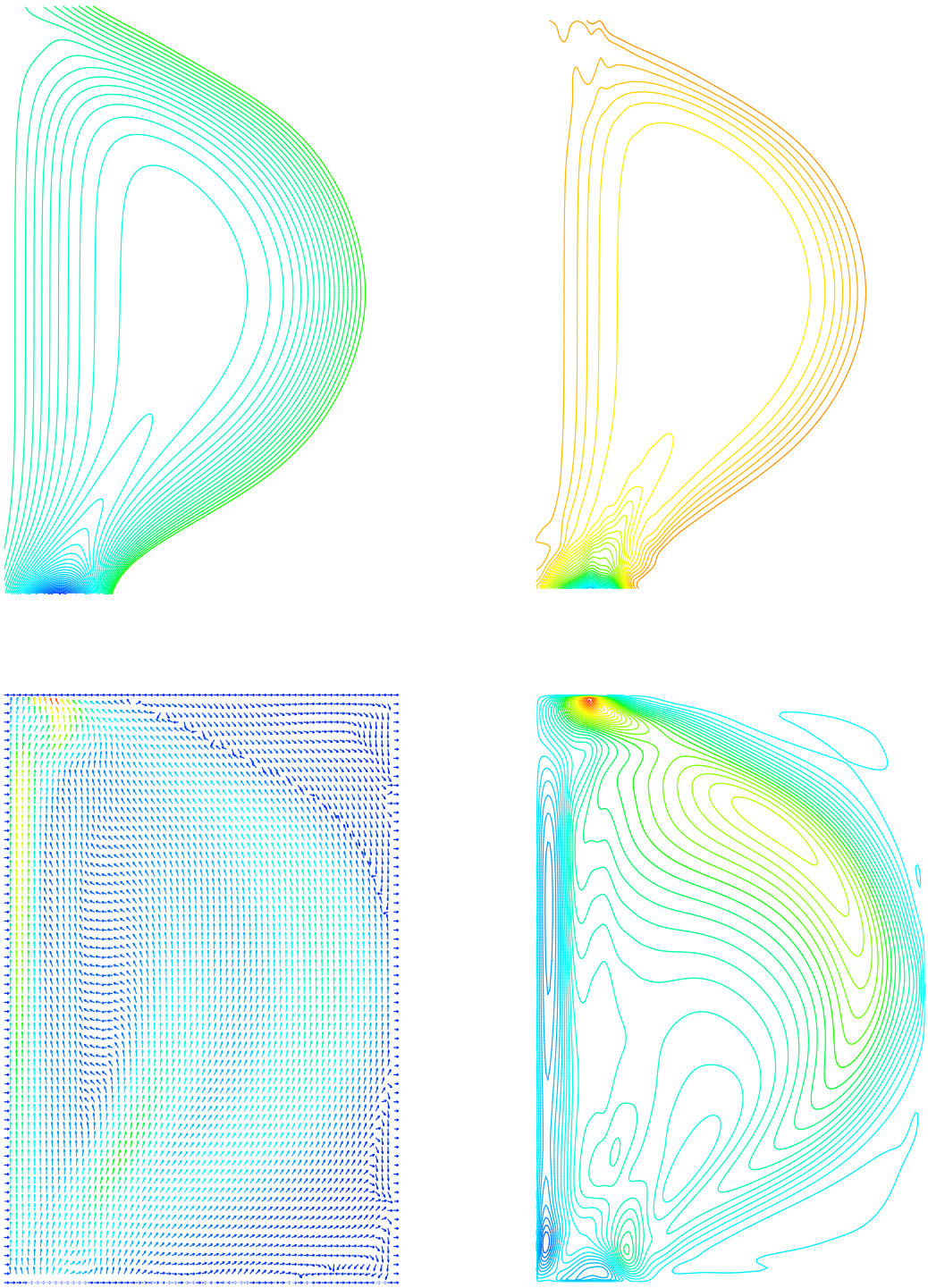

Figure 2: Top left: poloidal flux ψ; top right: RB_φ; Bottom left: poloidal flow; Bottom right: v_φ.

Resistive Steady State: $\mathbf{j}_\perp$

- $\mathbf{j}_\perp$ is required for force balance with plasma inertia and viscous force,

$$\mathbf{j} \times \mathbf{B} = \mathbf{F}; \;\; \mathbf{F} = \rho \mathbf{v} \cdot \nabla \mathbf{v} - \rho \nu \nabla^2 \mathbf{v}.$$

- Largest $\mathbf{j}_\perp$ occurs around the absorber and injector with electrode gap d,

$$j_\perp \sim P_g^2 B/d, \;\; P_g \equiv \frac{v_{\mathbf{E}\times\mathbf{B}}}{v_A} = g\frac{\rho^{1/2}\mathcal{V}}{dB^2}.$$

  Plasma gun parameter P_g depends on a geometric factor $g \sim 1 - \mathbf{E}\cdot\mathbf{B}/EB$.

- At the injector, poloidal field is designed to be maximumly aligned with $\mathbf{E}$ for high efficiency in driving the parallel current ($g \to 0$). Opposite is true at the absorber ($g \to 1$).

Resistive Steady State: $j_{\|}$

- Parallel current is the one affected most by flows,

$$k_{\|} \equiv \mathbf{j} \cdot \mathbf{B}/jB = k_n(\psi) + k_{ps}(\psi, \theta) + k_{\alpha\psi}(\psi, \theta).$$

- Net parallel current $k_n(\psi)$ is not affected by $\mathbf{j}_{\perp}$ or

$$\mathbf{F} = F_{\psi}(\psi, \theta)\nabla\psi + F_{\alpha}(\psi, \theta)\nabla\alpha.$$

  Clebsch coordinates $\alpha \equiv \theta - \iota\varphi, \xi \equiv \theta + \iota\varphi$.

- Pfirsch-Schlüter current is driven by F_{ψ},

$$k_{ps} = \frac{2g_{\alpha\xi}}{qJ_m B^2} F_{\psi} - \frac{qJ_m}{2} F_{\psi}.$$

- $k_{\alpha\psi}$ current is driven by F_{α},

$$k_{\alpha\psi} = -\frac{2g_{\psi\xi}}{qJ_m B^2} F_{\alpha} + \int_0^{\theta} \frac{\partial}{\partial\psi}(qJ_m F_{\alpha}) d\theta'.$$

Small $k_\perp \rightarrow$ large $k_\parallel$

- Normalized perpendicular current and magnetic field

$$k_\perp^\alpha \equiv \frac{\mathbf{j}_\perp \cdot \nabla\alpha}{\sqrt{g^{\alpha\alpha}}B} = \frac{F_\psi}{\sqrt{g^{\alpha\alpha}}B} \quad ; \quad k_\perp^\psi \equiv \frac{\mathbf{j}_\perp \cdot \nabla\psi}{\sqrt{g^{\psi\psi}}B} = -\frac{F_\alpha}{\sqrt{g^{\psi\psi}}B}.$$

$$b_\alpha = \mathbf{B} \cdot \frac{\partial \mathbf{x}}{\partial\alpha}/B\sqrt{g_{\alpha\alpha}} \quad ; \quad b_\psi = \mathbf{B} \cdot \frac{\partial \mathbf{x}}{\partial\psi}/B\sqrt{g_{\psi\psi}}.$$

- Pfirsch-Schlüter current $\sim q^2 k_\perp^\alpha$

$$k_{ps} = b_\alpha\sqrt{g_{\alpha\alpha}g^{\alpha\alpha}}k_\perp^\alpha - \frac{1}{2}qJ_m\sqrt{g^{\alpha\alpha}}Bk_\perp^\alpha$$

- $k_{\alpha\psi}$ current $\sim \frac{\partial}{\partial\psi}(qJ_mB\sqrt{g^{\psi\psi}})k_\perp^\psi$.

$$k_{\alpha\psi} = b_\psi\sqrt{g_{\psi\psi}g^{\psi\psi}}k_\perp^\psi - \int_0^\theta \frac{\partial}{\partial\psi}(qJ_m\sqrt{g^{\psi\psi}}Bk_\perp^\psi)d\theta'$$

- Strong parallel current is localized poloidally around injector where local B_θ is small on a high q field line, and around absorber where local B_θ is strong on a high q field line near the X point.

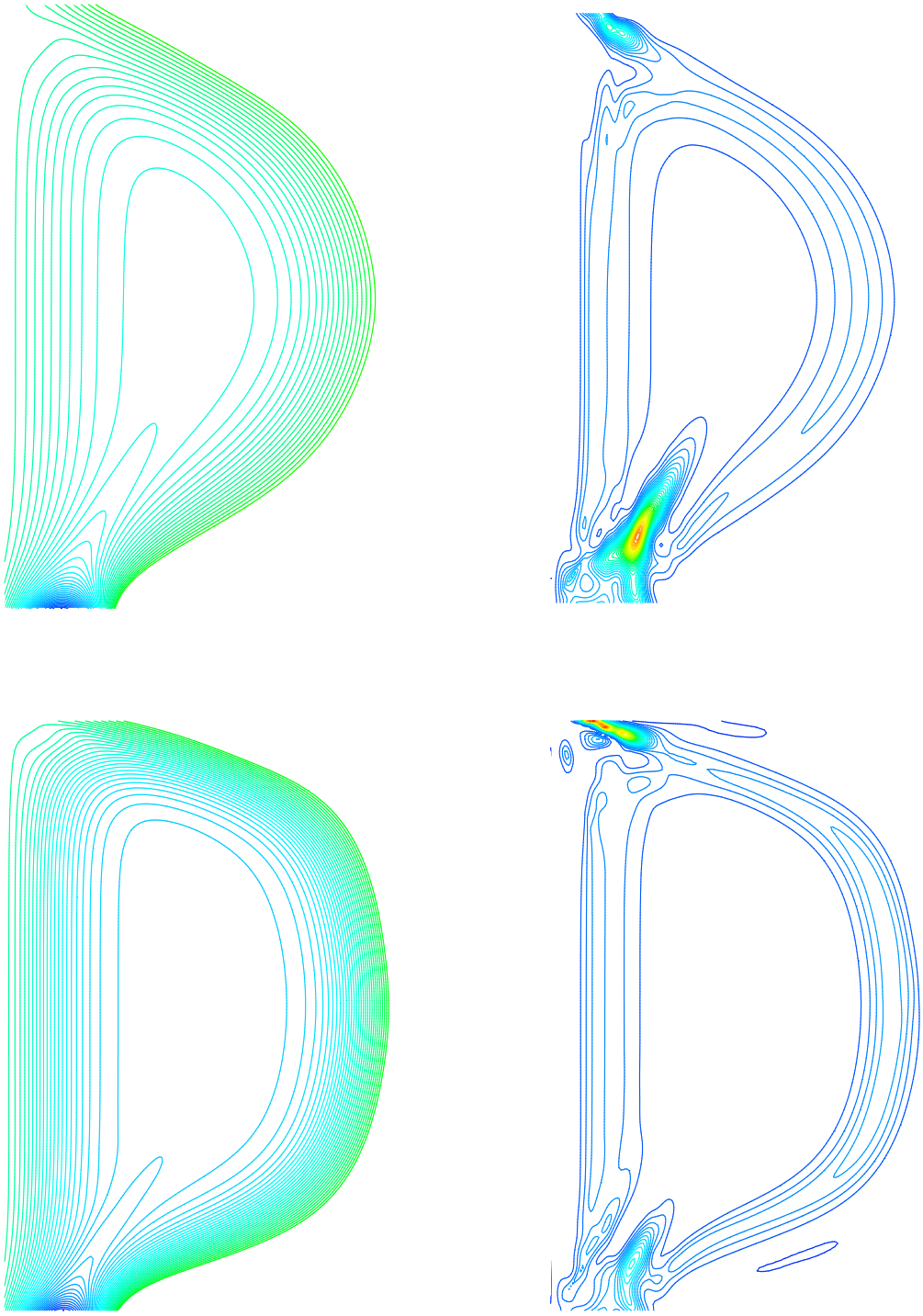

Figure 3: Left: poloidal flux ψ; right: k_n. Bottom run has twice the voltage as the top run. In both cases, $k_n \gg k_\perp$.

3D instability and nonlinear saturation

- The generic state of an electro-statically driven plasma has peaked edge current density, a strong drive for kink modes. (Requires vacuum open field line region to operate efficiently)

- Line-tied kink can be ideally unstable, but magnetic topology can only change due to non-ideal effect, such as resistivity.

- Depends on the drive, resistivity, and other factors, the saturated nonlinear states can be very different. (characterized by the $n = 0$ component).

- The saturated nonlinear state tends to be time dependent. The time history of the diagnostic signals can be used to decipher the internal MHD dynamics.

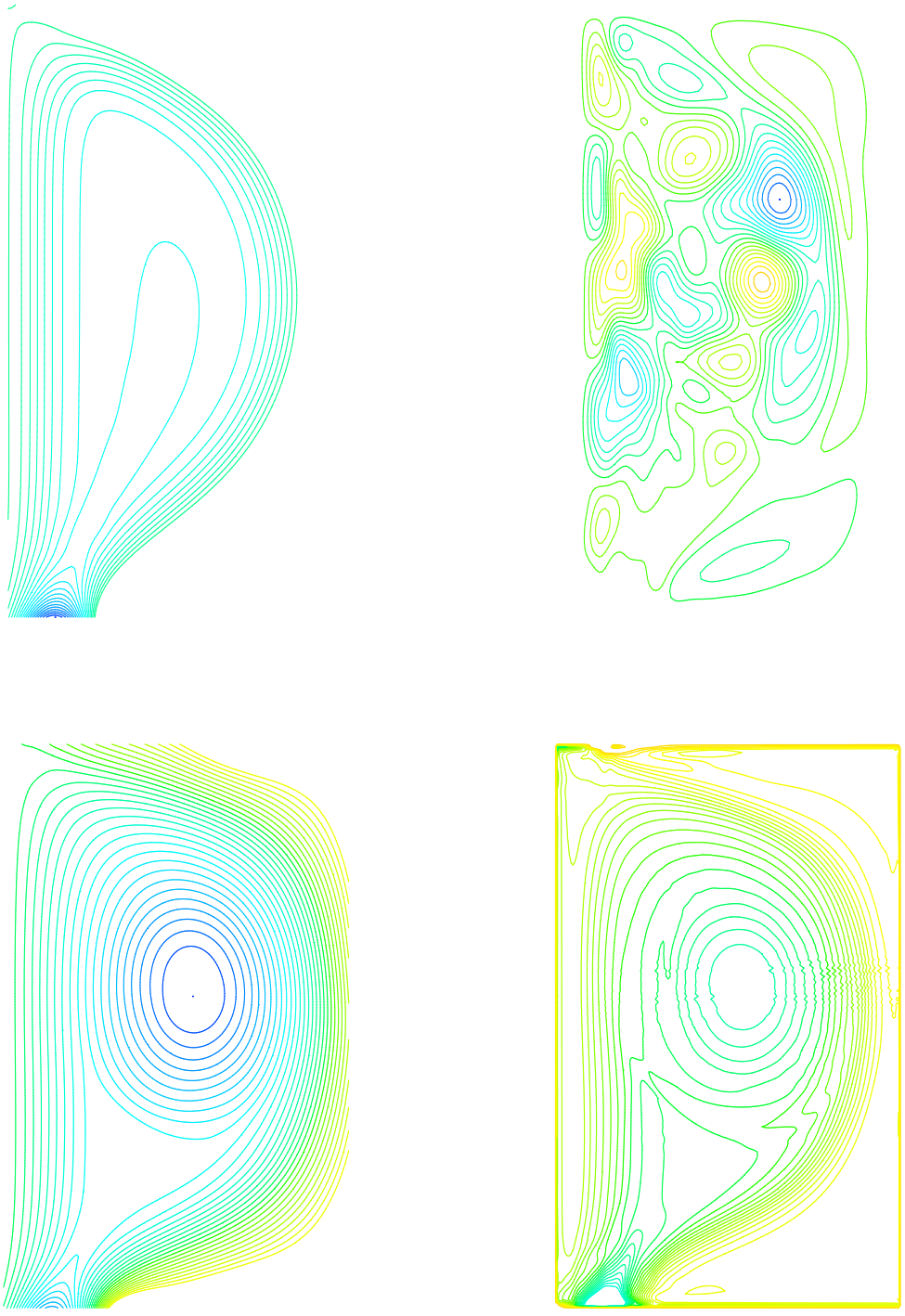

Figure 4: Top left: Axisymmetric steady state χ; Top right: n=1 component of 3D χ; Bottom left: $n = 0$ component of 3D χ; Bottom right: $n = 0$ component of 3D RB_φ.

Transient CHI for secondary current drive

- Non-inductive startup is attractive for NSTX and future ST devices.

- CHI prepares the initial plasma and field. Secondary current drive provides profile control and sustainment.

- Secondary current drive (Ohmic, beam, rf wave) all require a plasma core with adequate confinement (closed flux surfaces).

- Steady state CHI plasma with good core confinement remains an issue of debate, but transient CHI plasma can easily satisfy the requirement.

2D or 3D?

- Transient axisymmetric CHI plasma: forced 2D reconnection to form large volume of axisymmetric plasmoid.
  - pinching off the injector flux or modulating the voltage.
  - downside: q profile is opposite of eventual ST profile, more work for secondary drive.

- Transient 3D CHI plasma: ramp-down a nonlinearly saturated high-$\mathcal{V}$ 3D plasma.
  - saturated $n = 0$ component has substantial current penetration into the core.
  - fast decay of $n > 0$ modes leaves $n = 0$ with ST-like q profile.
  - room for q profile optimization during the CHI phase.

- Details will be presented at APS/DPP'2002.